BPM-CUL3 E3 ligase modulates thermotolerance by facilitating negative regulatory domain-mediated degradation of DREB2A in *Arabidopsis*

Kyoko Morimoto[a,1,2], Naohiko Ohama[a,1,3], Satoshi Kidokoro[a], Junya Mizoi[a], Fuminori Takahashi[b], Daisuke Todaka[a], Junro Mogami[a], Hikaru Sato[a], Feng Qin[c,4], June-Sik Kim[b], Yoichiro Fukao[d], Masayuki Fujiwara[d], Kazuo Shinozaki[b], and Kazuko Yamaguchi-Shinozaki[a,5]

[a]Laboratory of Plant Molecular Physiology, Graduate School of Agricultural and Life Sciences, The University of Tokyo, Bunkyo-ku, Tokyo 113-8657, Japan; [b]Gene Discovery Research Group, RIKEN Center for Sustainable Resource Science, Yokohama, Kanagawa 230-0045, Japan; [c]Biological Resources and Post-Harvest Division, Japan International Research Center for Agricultural Sciences, Tsukuba, Ibaraki 305-8686, Japan; and [d]Plant Global Education Project, Graduate School of Biological Sciences, Nara Institute of Science and Technology, Ikoma, Nara 630-0192, Japan

Edited by Julia Bailey-Serres, University of California, Riverside, CA, and approved August 22, 2017 (received for review March 13, 2017)

DEHYDRATION-RESPONSIVE ELEMENT BINDING PROTEIN 2A (DREB2A) acts as a key transcription factor in both drought and heat stress tolerance in *Arabidopsis* and induces the expression of many drought- and heat stress-inducible genes. Although *DREB2A* expression itself is induced by stress, the posttranslational regulation of DREB2A, including protein stabilization, is required for its transcriptional activity. The deletion of a 30-aa central region of DREB2A known as the negative regulatory domain (NRD) transforms DREB2A into a stable and constitutively active form referred to as DREB2A CA. However, the molecular basis of this stabilization and activation has remained unknown for a decade. Here we identified BTB/POZ AND MATH DOMAIN proteins (BPMs), substrate adaptors of the Cullin3 (CUL3)-based E3 ligase, as DREB2A-interacting proteins. We observed that DREB2A and BPMs interact in the nuclei, and that the NRD of DREB2A is sufficient for its interaction with BPMs. *BPM*-knockdown plants exhibited increased DREB2A accumulation and induction of DREB2A target genes under heat and drought stress conditions. Genetic analysis indicated that the depletion of *BPM* expression conferred enhanced thermotolerance via DREB2A stabilization. Thus, the BPM-CUL3 E3 ligase is likely the long-sought factor responsible for NRD-dependent DREB2A degradation. Through the negative regulation of DREB2A stability, BPMs modulate the heat stress response and prevent an adverse effect of excess DREB2A on plant growth. Furthermore, we found the BPM recognition motif in various transcription factors, implying a general contribution of BPM-mediated proteolysis to divergent cellular responses via an accelerated turnover of transcription factors.

abiotic stress response | co-IP coupled with LC-MS/MS | DREB2A-interacting proteins | E3 ubiquitin ligase | posttranslational regulation

Plants often manage to survive under various environmental stress conditions, such as drought, high salinity, and extreme temperatures. Transcriptional regulation is one of the most important mechanisms in the acquisition of stress tolerance (1, 2). However, in many cases, stress adaptation is exchanged for growth and productivity; therefore, it is necessary for plants to develop a resilient system to obtain the optimal trade-off for survival and growth. To this end, plants use elaborate mechanisms associated with posttranscriptional modulation (3) and posttranslational regulation (4–6), as well as transcriptional regulation. In particular, the appropriate control of transcription factors regulating stress-inducible genes is important, because these transcription factors negatively affect plant growth and productivity while being essential for increased stress tolerance. The environmental conditions surrounding plants are constantly changing; thus, posttranslational regulation to control the protein levels of these transcription factors is considered an important mechanism to avoid adverse effects on plant growth and productivity.

DEHYDRATION-RESPONSIVE ELEMENT-BINDING PROTEIN 2A (DREB2A), an APETALA2/ethylene-responsive element binding factor-type (AP2/ERF) transcription factor, is a key factor governing the expression of many target genes in response to drought and heat stresses via a *cis*-acting element known as the dehydration-responsive element/C-repeat (DRE/CRT; A/GCCGAC) (7). Expression of the *DREB2A* gene itself is induced by these stresses via different *cis*-acting elements in its promoter region (8, 9); however, the expression of *DREB2A* alone is not sufficient to activate the expression of DREB2A target genes, reflecting a posttranslational negative regulatory system (10). The posttranslational regulation of DREB2A involves the control of protein stability mediated by the 30-aa negative regulatory domain

Significance

DEHYDRATION-RESPONSIVE ELEMENT-BINDING PROTEIN 2A (DREB2A) is a key transcription factor for plant adaptation to drought and heat. DREB2A activity is strictly regulated via proteolysis mediated by the negative regulatory domain (NRD), although the molecular basis for this regulation has remained unclear for a decade. We reveal that BTB/POZ AND MATH DOMAIN proteins (BPMs), substrate adaptors for Cullin3-based E3 ubiquitin ligase, are the long-sought factors responsible for NRD-dependent DREB2A degradation. Through DREB2A degradation, BPMs negatively regulate the heat stress response and prevent the adverse effects of excess DREB2A on plant growth. Furthermore, we found the BPM recognition motif in various transcription factors, implying a general contribution of BPM-mediated proteolysis to divergent cellular responses via an accelerated turnover of transcription factors.

Author contributions: K.M., N.O., K.S., and K.Y.-S. designed research; K.M., N.O., S.K., J. Mizoi, D.T., J. Mogami, H.S., and F.Q. performed research; F.T., Y.F., and M.F. contributed new reagents/analytic tools; S.K., J. Mizoi, F.T., and J.-S.K. analyzed data; and K.M., N.O., and K.Y.-S. wrote the paper.

The authors declare no conflict of interest.

This article is a PNAS Direct Submission.

Data deposition: Microarray data have been deposited in the European Bioinformatics Institute's ArrayExpress database, www.ebi.ac.uk/arrayexpress/ (accession no. E-MTAB-5845).

[1]K.M and N.O. contributed equally to this work.

[2]Present address: The Plant Chemetics Laboratory, Department of Plant Sciences, University of Oxford, Oxford OX1 3RB, United Kingdom.

[3]Present address: Temasek Life Sciences Laboratory, National University of Singapore, Singapore 117604, Singapore.

[4]Present address: State Key Laboratory of Plant Physiology and Biochemistry, College of Biological Sciences, China Agricultural University, Beijing 100193, China.

[5]To whom correspondence should be addressed. Email: akys@mail.ecc.u-tokyo.ac.jp.

This article contains supporting information online at www.pnas.org/lookup/suppl/doi:10.1073/pnas.1704189114/-/DCSupplemental.

(NRD) adjacent to the ERF/AP2 DNA-binding domain. Removal of the NRD yields a constitutively stable and active form of DREB2A known as DREB2A CA. Overexpression of DREB2A CA induces the expression of DREB2A target genes, even under control conditions, and enhances tolerance to drought and heat stresses (10, 11). At the same time, overexpression of DREB2A CA also adversely affects plant growth, resulting in dwarfism and reduced reproduction. Therefore, NRD-mediated negative regulation contributes to avoidance of the adverse effects of DREB2A induction through the strict control of its stability. However, despite the importance of DREB2A in stress responses, the molecular basis of NRD function has been unclear for a decade.

DREB2A-INTERACTING PROTEINS 1 and 2 (DRIP1/2) are C3HC4 RING domain-containing proteins identified as DREB2A interactors that function as E3 ubiquitin ligases (12). Through the acceleration of 26S proteasome-mediated DREB2A proteolysis, DRIP1/2 negatively regulate the expression of DREB2A-downstream genes. However, double knockout of *DRIP1/2* was found to only partially enhance the stability of DREB2A under stress conditions (13). Therefore, other E3 ligases have been implicated in DREB2A degradation.

Cullin-RING ubiquitin ligases (CRLs) are a well-studied family of multisubunit E3 ligases in eukaryotes (14). Plants have three types of Cullins: CUL1/CU2a/b, CUL3a/b, and CUL4 (15). These molecules function as scaffold proteins that assemble a complex containing RING-BOX (RBX)-1, an adaptor for E2, and a variety of receptors recognizing specific substrates for ubiquitylation. Broad complex, tram track, bric-a-brac/Pox virus, and zinc finger (BTB/POZ) domain-containing proteins function as the substrate receptors for CUL3-based CRL (CRL3) (16). Among the 80 BTB/POZ domain-containing proteins in *Arabidopsis*, six are known as BTB/POZ AND MEPRIN AND TRAF HOMOLOGY (MATH) DOMAIN (BPM) proteins. BPM1–BPM6 (BPM1-6) interact with and modulate the turnover of various transcription factors belonging to distinct families, such as WRI1, ATHB6, and MYB56 (17–19). Through the regulation of these transcription factors, BPMs are involved in the control of fatty acid metabolism, the abscisic acid (ABA) response, and flowering (17–19).

In the present study, to further elucidate the posttranslational regulatory mechanism of DREB2A, we performed coimmunoprecipitation (co-IP) coupled with liquid chromatography–tandem mass spectrometry (LC-MS/MS) analysis to identify the components of DREB2A-associated protein complexes. We isolated and characterized BPMs as novel DREB2A interactors and observed that BPMs recognize and destabilize DREB2A via the NRD. Knockdown of *BPMs* resulted in accumulation of the DREB2A protein and hyperactivation of the DREB2A target genes under stress conditions. These results suggest that the BPM-CUL3 E3 ligase ($CRL3^{BPM}$) is the long-sought factor responsible for the destabilization of DREB2A via the NRD, orchestrating the response to drought and heat stresses through the control of DREB2A stability.

Results

Identification of BPM2 as a DREB2A-Interacting Protein. To investigate the posttranslational regulatory mechanism of DREB2A, we identified DREB2A-interacting proteins through co-IP coupled with LC-MS/MS analysis using *35S:GFP-DREB2A/dreb2a* transgenic plants (13). DREB2A and its interactors were purified from heat-stressed plants using an anti-GFP antibody (Fig. S1*A*), and 37 proteins were specifically identified in the GFP-DREB2A fraction by LC-MS/MS analysis (Dataset S1). The identification of RCD1, which has been reported as a DREB2A-interacting protein (20), indicates that this screening system is valid. After excluding proteins predicted to be localized to the plastid, mitochondrion, or plasma membrane as false-positives, we focused on proteins related to protein degradation (BPM2 and BPM4) (21), protein folding (TCP1) (22), and transcriptional regulation (SAP18) (23) as the putative regulators of DREB2A activity. We confirmed the interactions of candidate proteins and RCD1 with DREB2A using a yeast two-hybrid (Y2H) assay. Yeast growth on the agar plate (Fig. 1*A*) and in the liquid medium (Fig. S1*B*) indicates that BPM2 and BPM4 interact with DREB2A, but TCP1 and SAP18 do not. Thus, we selected BPM2 and BPM4 as potential DREB2A interactors for further analysis.

Although BPM2 and BPM4 were predicted to be localized to the cytosol (Dataset S1), BPM2 is reportedly localized to the nucleus in tobacco (24). To reveal the accurate localization of BPM2 and BPM4 in *Arabidopsis*, we generated overexpressors of GFP-fused BPM2 and BPM4. BPM2 was localized in the nucleus under both normal and heat stress conditions, whereas BPM4 translocated from the cytosol to the nucleus on heat shock (Fig. 1*B*). The GFP-DREB2A signal was observed in the nucleus only after heat stress. Taken together, our findings indicate that both BPM2 and BPM4 are localized in the nucleus under heat stress conditions, suggesting that they potentially colocalize and interact with DREB2A in vivo.

To examine the interactions between BPMs and DREB2A in living cells, we conducted a bimolecular fluorescence complementation (BiFC) assay with onion epidermal cells. Before the assay, we assessed the subcellular localization of these proteins in this expression system. DREB2A and BPM2 were clearly localized in the nucleus, while the fluorescence of GFP-BPM4 in the nucleus was obscure regardless of heat shock (Fig. S1*C*). In the BiFC assay, we did not observe any signal using a combination of DREB2A and full-length BPMs (Fig. S1*D*), likely reflecting the fact that BPMs are involved in protein degradation as the substrate adaptors of CRL3. The DREB2A-BPM complex may be rapidly degraded, making it difficult to observe the interaction signal. To overcome this problem, we generated BPMs lacking a BTB domain (the CUL3-interaction domain). A YFP signal was clearly observed in the nucleus when a combination of DREB2A and BPM2_ΔB was used. In contrast, an interaction between DREB2A and BPM4 was not observed, likely reflecting the difference in subcellular localization between DREB2A and BPM4 (Fig. S1*C*). To mimic the heat-inducible nuclear accumulation of BPM4, we generated a nuclear-accumulating form of BPM4_ΔB (BPM4_ΔB-NLS). BPM4_ΔB-NLS localized to the nucleus and interacted with DREB2A (Fig. S1 *E* and *F*). Thus, both BPM2 and BPM4 can interact with DREB2A in the nucleus. The constitutive nuclear localization of BPM2 indicates that BPM2 is the major BPM interacting with DREB2A. Therefore, in the subsequent analysis, we focused primarily on BPM2 as a representative BPM.

To further examine the interaction between BPM2 and DREB2A, we performed a pull-down assay and co-IP. In the pull-down assay, Trx-6xHis-DREB2A protein was pulled down by GST-BPM2 (Fig. S1*G*), indicating direct physical interaction between these proteins. Co-IP was performed under the same conditions used in the co-IP for LC-MS/MS analysis. BPM2 was specifically coimmunoprecipitated with DREB2A from the transgenic *Arabidopsis* plants overexpressing streptavidin-3×FLAG (NSF)-tagged BPM2 and GFP-DREB2A (Fig. 1*C*). Conversely, endogenous DREB2A was coimmunoprecipitated with BPM2 from the transgenic plants overexpressing GFP-BPM2 in the wild-type (WT) background (Fig. 1*D*). These data consistently support the direct interaction between BPM2 and DREB2A in vivo.

BPMs Interact with DREB2A via the NRD. We conducted additional Y2H assays to identify the domain of DREB2A necessary for the interaction with BPM2. Several DREB2A fragments were designed based on conserved domains, including the AP2/ERF DNA-binding domain (AP2), the NRD, and the activation domain (AD; Fig. 2*A*). The results show that the NRD is sufficient for the interaction with BPM2 (Fig. 2*A* and Fig. S2*A*). To narrow

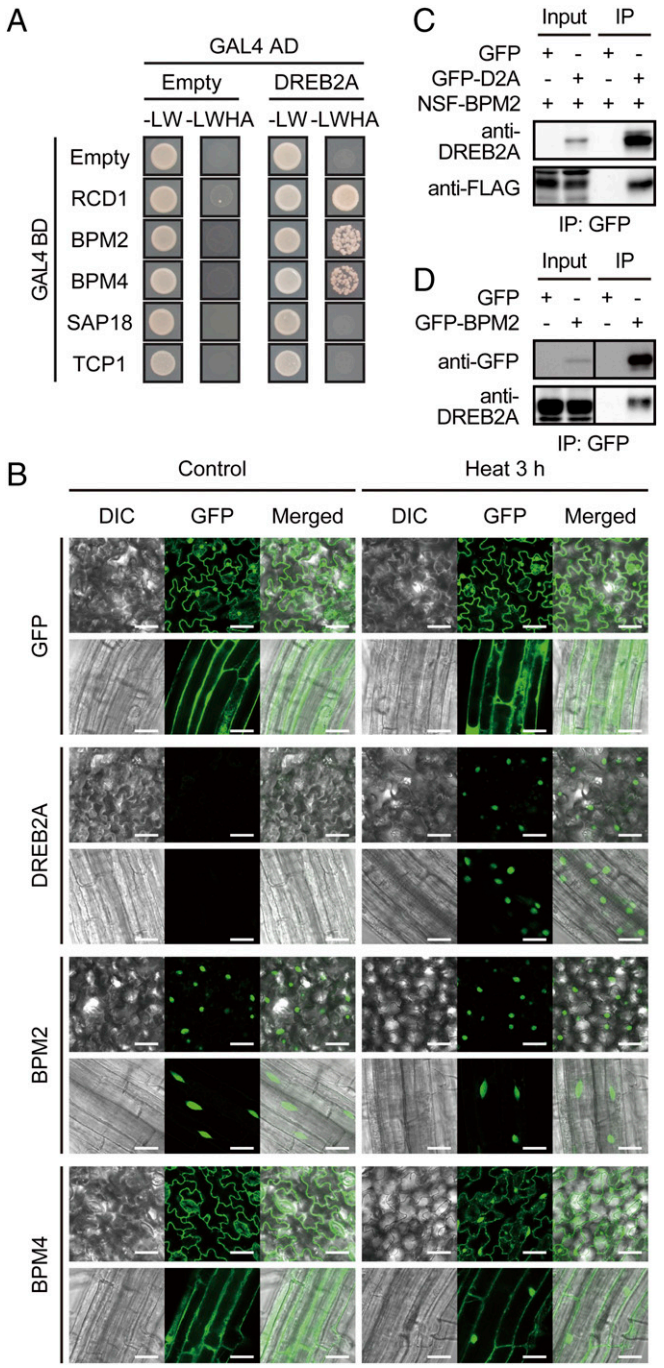

Fig. 1. BPM2 is a DREB2A-interacting protein. (*A*) Validation of interactions between DREB2A and the candidate interactors by Y2H assay. The growth of yeast strains on nonselective medium (–LW) and selective medium (–LWHA) is shown. (*B*) Subcellular localization of DREB2A, BPM2, and BPM4 in transgenic plants under normal and heat stress conditions. These plants express N-terminal GFP-fused proteins under the control of the *35S* promoter. (*Upper*) Images of true leaves. (*Lower*) Images of roots. Differential interference contrast (DIC) and GFP fluorescence images as well as merged images are shown. (Scale bars: 20 μm.) (*C* and *D*) Validation of interaction between DREB2A and BPM2 by co-IP from transgenic plants either co-overexpressing *NSF-BPM2* and *GFP-DREB2A* (GFP-D2A) in the background of the *dreb2a* mutant (*C*) or overexpressing *GFP-BPM2* in the WT background (*D*).

down the interacting region in the NRD, we divided the NRD into N-terminal (N-NRD) and C-terminal (C-NRD) halves and found that the N-NRD is necessary and sufficient for the interaction between DREB2A and BPM2 (Fig. 2*A* and Fig. S2*A*). The V-T-S-T-S amino acid sequence in N-NRD corresponds to the speckle-type POZ protein (SPOP)-binding consensus (SBC) motif, ϕ-π-S-S/T-S/T (ϕ, nonpolar; π, polar; Fig. 2*B*) (25). SPOP is the BPM ortholog in humans. To reveal whether the SBC motif is important for the recognition of N-NRD by BPM2, we examined the interaction between BPM2 and an SBC motif-mutated N-NRD. Although the T145 mutation did not affect the interaction, replacement of S144 or S146 with alanine blocked BPM2 binding (Fig. 2*B* and Fig. S2*B*), indicating the importance of the SBC motif in the interaction between DREB2A and BPM2. This result implies that BPM2 recognizes not only the perfect SBC motif, but also the SBC-like motif, ϕ-π-S-X-S/T (X, any amino acid). Thus, we searched all of the proteins reported to interact with BPMs for these motifs (17–19, 24), and found that most of these proteins contain SBC or SBC-like motifs (Fig. S2*C*).

Conversely, we also identified the domain of BPM2 that recognizes the NRD. BPMs possess two conserved domains, the MATH domain and the BTB/POZ domain (Fig. S2*D*), which function as a substrate-recognition domain and a CUL3-interaction domain, respectively (24). We generated a truncated

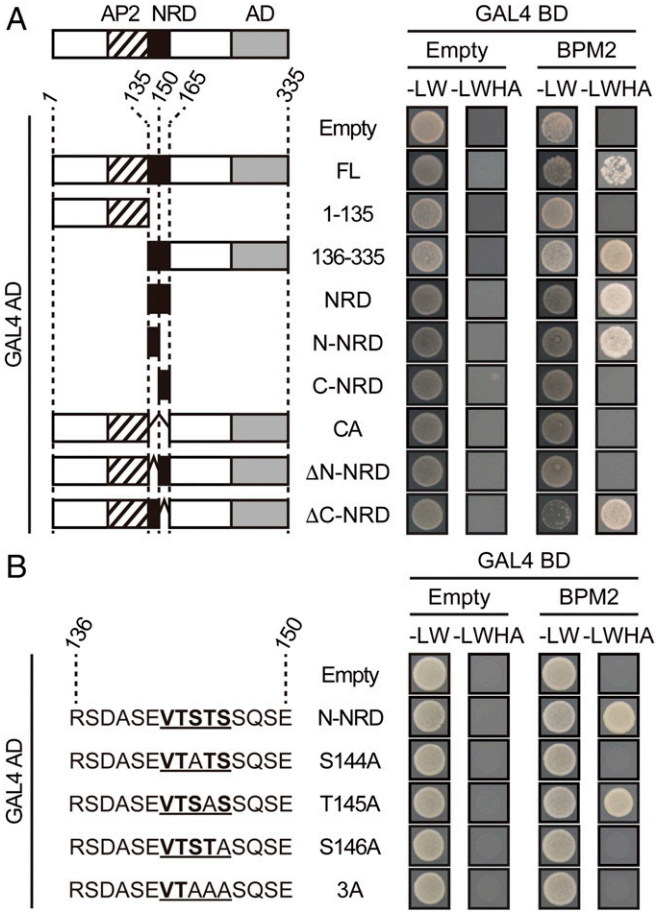

Fig. 2. BPM2 interacts with DREB2A by recognizing the SBC motif in NRD. (*A*) Identification of the BPM2-interacting domain in DREB2A using a Y2H assay. (*Left*) Schematic diagram of the DREB2A fragments. The numbers indicate the corresponding amino acid residues. AP2, DNA-binding domain; NRD, negative regulatory domain; AD, activation domain; FL, full-length DREB2A; CA, DREB2A CA. (*B*) Mutation analysis of the SBC motif. (*Left*) Amino acid sequences of the preys. Underscored bold letters represent the potential SBC motif, and underscored regular letters indicate the mutated residues.

form of BPM2 lacking either the MATH domain (ΔMATH) or the BTB/POZ domain (ΔBTB). Consistent with the functions of each domain, the MATH domain was necessary for the interaction between BPM2 and the NRD (Fig. S2*D*). To examine whether BPMs other than BPM2 also recognize the NRD, we performed a Y2H assay with all BPMs and found that all of the BPMs interacted with the NRD (Fig. S2*E*). To examine the interaction between DREB2A and BPMs in vivo, we performed a BiFC assay using BPMs lacking the BTB domain (Fig. S2*F*). A YFP signal was observed in the nucleus in the presence of DREB2A in combination with each of the BPMs. Taken together, these findings indicate that all BPMs have the potential to interact with DREB2A via the NRD.

DRIP1/2 are DREB2A interactors that function as E3 ubiquitin ligases (12). To examine whether the interaction domains of DREB2A overlap between DRIP1/2 and BPM2, we performed a Y2H assay using DREB2A fragments: an N-terminal fragment (DREB2A 1–135) and the NRD (Fig. S3 *A* and *B*). Both DRIP1 and DRIP2 interacted with DREB2A 1–135 but not with the NRD, while BPM2 specifically bound to the NRD. Thus, BPM2 and DRIP1/2 recognize distinct parts of DREB2A.

Knockdown of BPMs Causes Defects in DREB2A Degradation via the NRD. The NRD was identified as the BPM interaction domain of DREB2A (Fig. 2*A* and Fig. S2 *A* and *E*). Considering the function of BPMs as the substrate receptors of CRL3, these proteins might be the factors responsible for the NRD-mediated degradation of DREB2A. Thus, we sought to examine whether reduction of *BPM* expression affects DREB2A stability. Because all BPMs can interact with DREB2A (Fig. S2*E*), BPMs have the potential to redundantly function as destabilizers of DREB2A. To knock down all *BPMs* simultaneously, we generated overexpressors of an artificial microRNA (amiRNA) designed to target all *BPMs*. We obtained two independent transgenic lines with reduced *BPM* expression, and we refer to these transgenic plants as *amiBPM* (Fig. 3*A*).

To assess the effect of *BPM* knockdown on the activity and stability of DREB2A, we performed a transient expression assay using mesophyll protoplasts prepared from WT and *amiBPM* plants. We transfected the protoplasts with full-length DREB2A (FL), DREB2A CA (CA), DREB2A ΔN-NRD (ΔN), and DREB2A ΔC-NRD (ΔC). To estimate their transactivation activity, we cotransfected a construct consisting of three tandemly repeated DRE sequences fused to the *GUS* gene as a reporter (Fig. 3*B*). In WT protoplasts, ΔC exhibited reporter activity similar to that of the FL (Fig. 3*C*). In contrast, expression of ΔN increased activation of the reporter compared with FL; this activation level was similar to that of CA. However, in *amiBPM* protoplasts, the relative activity of FL and ΔC were significantly increased, indicating the negative effect of BPMs on DREB2A activity through N-NRD. We performed the same experiment with protoplasts derived from the *drip1 drip2* double mutant (Fig. S3*C*). In this case, the relative transactivation activity of the effectors was similar between WT and the *drip1 drip2* double mutant, indicating that DRIP1/2 are not responsible for the negative regulation via N-NRD. We subsequently analyzed the protein levels of DREB2A variants in WT and *amiBPM* protoplasts (Fig. 3 *D* and *E*), and found significantly increased relative protein levels of the FL and ΔC in *amiBPM* protoplasts. These data indicate that N-NRD destabilizes DREB2A in a BPM-dependent manner.

BPMs Are Involved in DREB2A Degradation Under Stress Conditions. To reveal the function of BPMs under stress conditions, we examined the accumulation of endogenous DREB2A in *amiBPM* plants under heat and drought stress conditions. Under heat stress at 37 °C, DREB2A accumulated within 3 h in the vector control (VC) plant, and its protein level then gradually decreased for up to

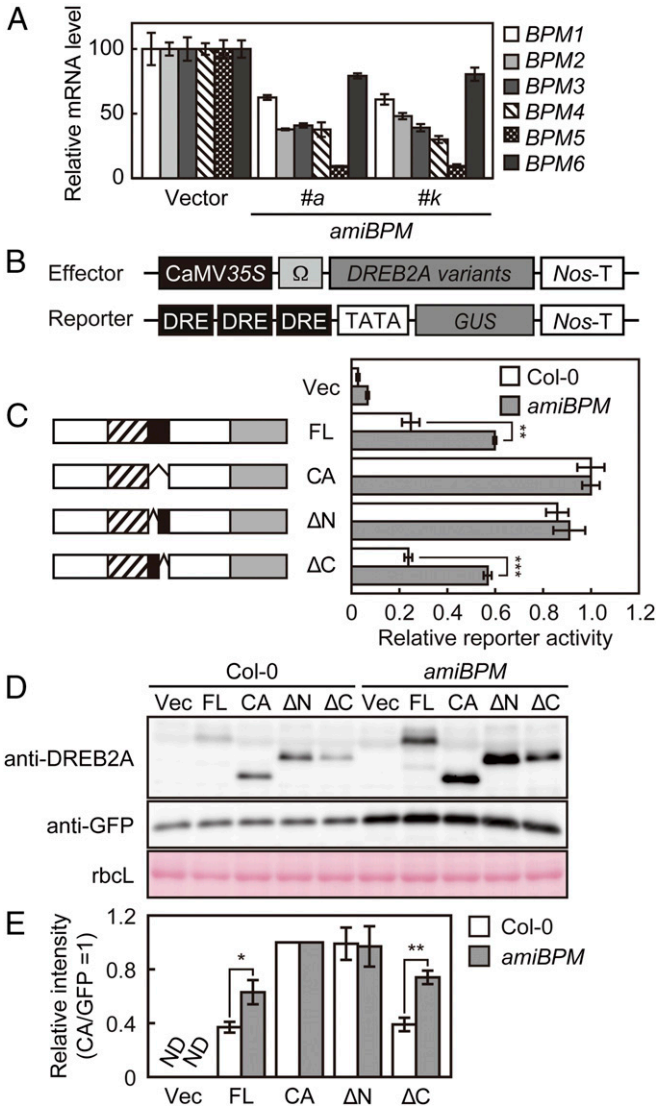

Fig. 3. Knockdown of *BPMs* leads to DREB2A accumulation in protoplasts. (*A*) Expression levels of *BPM1-6* in two *amiBPM* plants. The expression of *BPM* genes was determined through qRT-PCR analysis. The expression level of each *BPM* in VC was set to 100. The error bars indicate the SD from triplicate technical repeats. (*B*) Schematic diagram of the reporter and effector constructs. (*C*) Transactivation of the reporter gene by DREB2A variants. The error bars indicate the SD from three replicate samples. Asterisks indicate statistically significant differences between reporter activities: $^{**}P < 0.01$; $^{***}P < 0.001$, Student's *t* test. ΔN, DREB2A ΔN-NRD; ΔC, DREB2A ΔC-NRD. (*D* and *E*) Protein accumulation levels of DREB2A variants. The relative signal intensities of DREB2A variants normalized to the intensity of GFP are shown in (*E*). The signal intensity obtained with CA was set to 1. The error bars indicate the SD from triplicate experiments. Asterisks indicate significant differences between signal intensity: $^{*}P < 0.05$; $^{**}P < 0.01$, Student's *t* test. The Rubisco large subunit (rbcL) stained with Ponceau S is shown as a loading control.

10 h (Fig. 4*A*). In the two lines of *amiBPM* plants, DREB2A levels remained high for 10 h compared with those in VC plants. In contrast, under drought stress conditions, a significant increase in DREB2A accumulation in *amiBPM* plants was observed at 24 h (Fig. 4*B*). This air-dry treatment caused quick desiccation, and the water loss rates were similar among all genotypes between 3 and 24 h after stress treatment (Fig. S4*A*). We then compared DREB2A protein levels in the *amiBPM* plants with those in the *drip1 drip2* double-mutant plants under stress conditions. There was a higher level of DREB2A protein accumulation in both plant

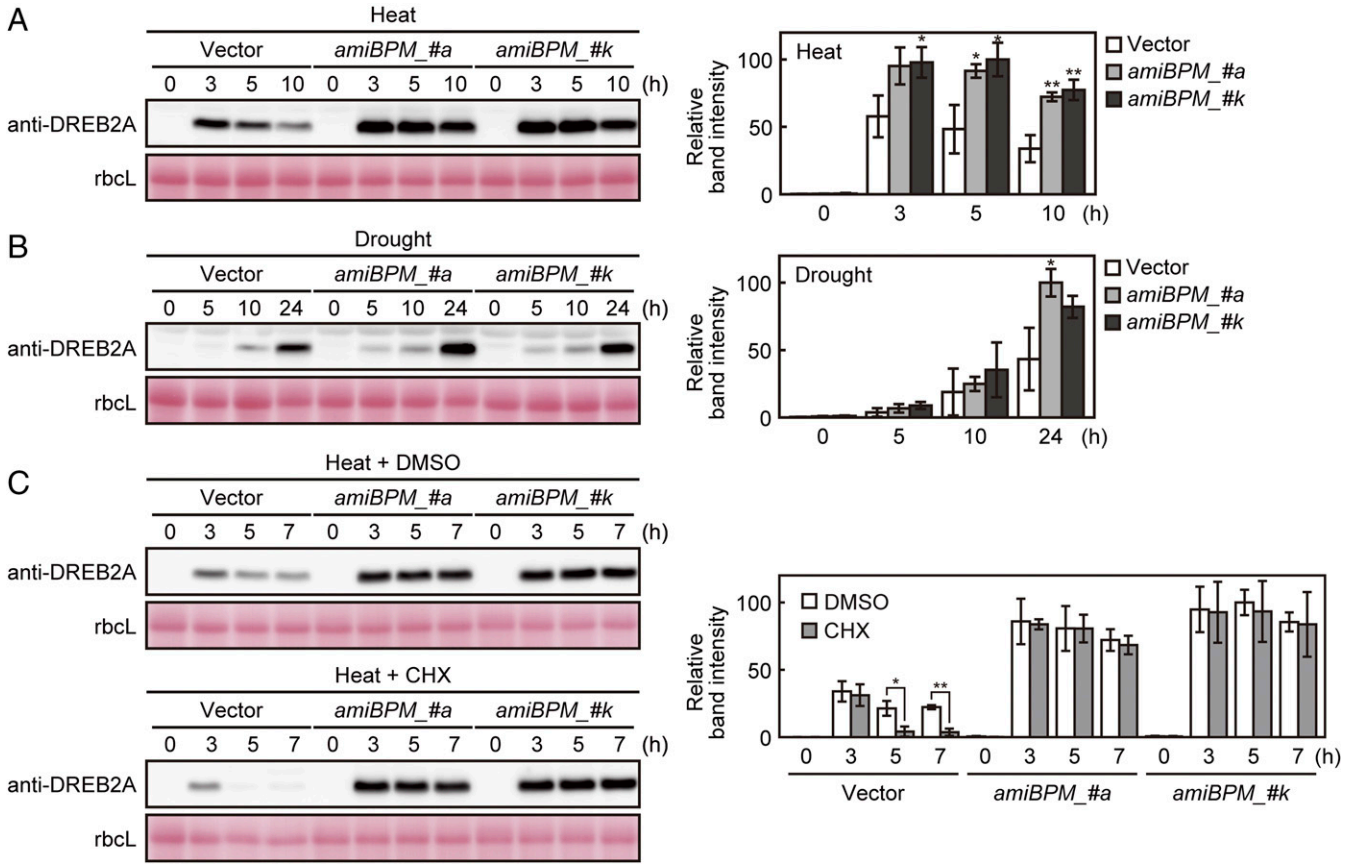

Fig. 4. DREB2A hyperaccumulates in the *amiBPM* plants grown on agar plates under stress conditions. (*A* and *B*) Accumulation levels of the DREB2A protein under heat (*A*) and drought (*B*) stress. (*Left*) Immunoblot analysis. (*Right*) Relative DREB2A band intensity of the immunoblot analysis. The highest intensity was set to 100. The error bars indicate the SD from triplicate experiments. Asterisks indicate significant differences compared with VC: $*P < 0.05$; $**P < 0.01$, Student's *t* test. (*C*) Accumulation of the DREB2A protein during heat stress treatment in the presence of DMSO or CHX. The error bars indicate the SD from triplicate experiments. Asterisks indicate significant differences of signal intensity between DMSO- and CHX-treated samples: $*P < 0.05$; $**P < 0.01$, Student's *t* test.

lines than in VC plants during heat stress treatment, while significant DREB2A accumulation was not observed in the *drip1 drip2* double-mutant plants during drought stress treatment (Fig. S4 *B* and *C*). In the *drip1 drip2* double-mutant plants, however, DREB2A was rapidly degraded during prolonged heat stress, and the amount of DREB2A reached the same level as that in VC plants within 24 h. In contrast, the *amiBPM* plants maintained higher DREB2A protein levels throughout the experiment. These results indicate that BPMs are the major factors that degrade DREB2A under stress conditions.

We assessed *DREB2A* expression levels in the *amiBPM* plants and found higher expression of this gene than that seen in VC plants (Fig. S4*D*). This result indicates that changes in expression are also potentially involved in the hyperaccumulation of DREB2A in *amiBPM* plants to some extent. Therefore, to demonstrate that DREB2A is truly stabilized at the protein level by knockdown of *BPMs*, we examined DREB2A stability in the presence of cycloheximide (CHX), an inhibitor of protein synthesis (Fig. 4*C*). CHX was added after 3 h of heat stress to achieve DREB2A accumulation, which strongly reactivated *DREB2A* expression within 2 h (Fig. S4*E*); however, the DREB2A protein was degraded in VC, indicating that CHX effectively inhibited the de novo synthesis of DREB2A (Fig. 4*C*). In contrast to VC, DREB2A protein levels in the *amiBPM* plants during CHX treatment were similar to those seen during dimethyl sulfoxide (DMSO) treatment. This result suggests that the DREB2A hyperaccumulation observed in *amiBPM* plants does not reflect changes in expression levels, but rather indicates changes in the protein stability of DREB2A.

BPMs Regulate Activity of the DREB2A Regulon and Modulate Thermotolerance. To analyze the effect of *BPM* knockdown on the DREB2A regulon, we examined the expression levels of several DREB2A target genes in the *amiBPM* plants. Heat-inducible (*HsfA3* and *At4g36010*) and drought-inducible (*RD29B* and *GolS1*) DREB2A target genes were strongly expressed in these plants under heat and drought stress conditions, respectively (Fig. 5 *A* and *B*). To reveal whether *BPM* knockdown specifically affects the DREB2A regulon among stress-inducible genes, we examined the transcriptome of the *amiBPM* plants under heat stress conditions. We did not use drought stress conditions in this experiment, because it has been reported that *BPM* knockdown causes stabilization of ATHB6, a negative regulator of ABA responses (18). Abnormal accumulation of ATHB6 disrupts ABA-responsive gene expression and stomatal closure, making it difficult to distinguish the effect of DREB2A accumulation on the transcriptomic change during drought treatment. After 5 h of heat stress, compared with their expression in the VC plants, 89 genes, including 20 heat-inducible genes, were up-regulated by more than 1.75-fold in the *amiBPM* plants (Fig. 5*C* and Dataset S2) (11). Importantly, 11 of these 20 heat-inducible genes were DREB2A target genes, and only one gene was a target gene of HsfA2, one of the major regulators of heat stress-inducible gene expression (Fig. 5*C* and Dataset S2) (11, 26). Hyperinduction of DREB2A target genes

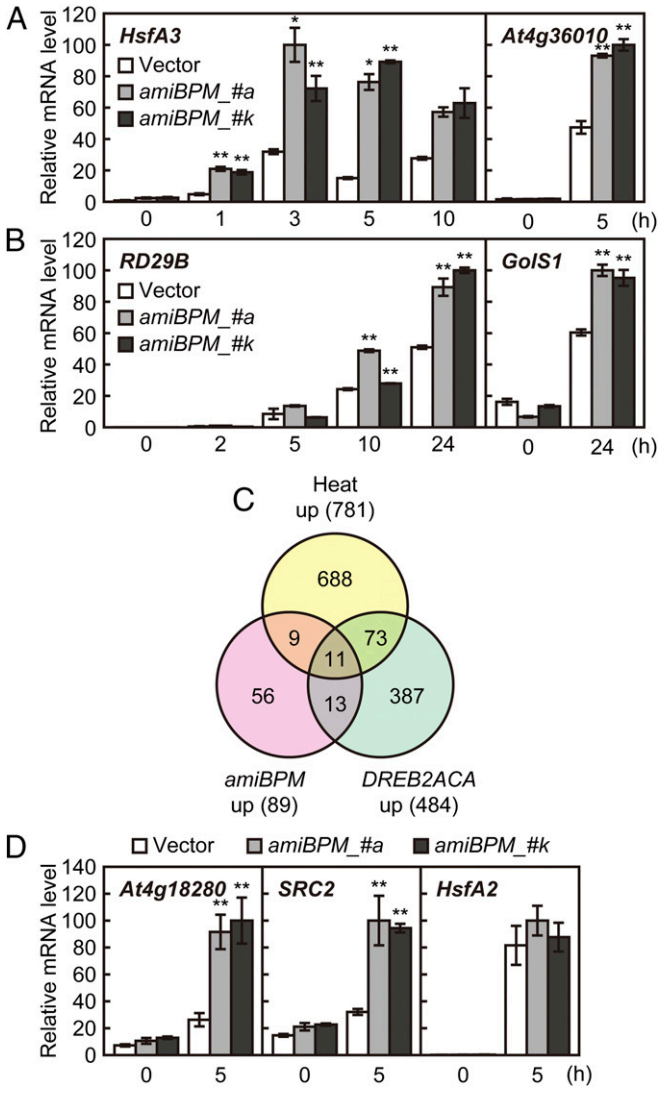

Fig. 5. Knockdown of *BPMs* enhances the expression of DREB2A target genes. (*A* and *B*) Expression levels of DREB2A downstream genes under heat (*A*) and drought (*B*) stress conditions determined through qRT-PCR. The highest expression level was set to 100 for each gene. The error bars indicate the SD from triplicate technical repeats. Asterisks indicate significant differences compared with VC: $*P < 0.05$; $**P < 0.01$, Student's *t* test. (*C*) Venn diagram comparing up-regulated genes among the heat stress-treated *amiBPM*, the heat stress-treated WT, and the *DREB2A CA* overexpressor. (*D*) Expression levels of DREB2A-downstream heat-inducible genes up-regulated in the microarray analysis. *HsfA2* is a negative control gene regulated via DREB2A-independent pathways. The error bars indicate the SD from triplicate technical repeats. Asterisks indicate significant differences compared with VC: $*P < 0.05$; $**P < 0.01$, Student's *t* test.

(*At4g18280* and *SRC2*) was confirmed by quantitative reverse-transcription PCR (qRT-PCR; Fig. 5*D*). This result indicates that *BPM* knockdown affects the heat stress response through specific activation of the DREB2A regulon.

Considering the activation of the DREB2A regulon in *amiBPM* plants during heat stress, we assumed that these plants would exhibit a higher tolerance to heat stress. In fact, the *amiBPM* plants grown on agar plates showed a higher survival rate and chlorophyll content after severe heat shock (Fig. 6 *A*–*C*). We also assessed the thermotolerance of these plants grown in soil. To prevent desiccation during the stress treatment, this experiment was performed under high humidity. The *amiBPM* plants also exhibited improved thermotolerance in this assay, as shown by a higher survival rate, higher chlorophyll content, and lower ion leakage after heat shock (Fig. 6 *D*–*G*). To demonstrate that the improvement in thermotolerance in the *amiBPM* plants is caused by the accumulation of DREB2A, we generated *BPM*-knockdown plants in the background of *dreb2a* (*amiBPM*/*dreb2a*; Fig. S5*A*). These plants showed neither hyperinduction of *HsfA3* nor enhanced thermotolerance compared with VC plants (Fig. S5 *B*–*E*). These results suggest that BPMs modulate thermotolerance through the regulation of DREB2A protein stability. We also performed a drought tolerance test with *amiBPM* plants. Despite the increased expression of *RD29B* and *GolS1* (Fig. 5*B*), these plants exhibited decreased drought tolerance compared with VC plants (Fig. S6 *A* and *B*). This result implies that in the *amiBPM* plants, the negative effect of ATHB6 stabilization has a greater impact than the positive effect of DREB2A stabilization.

Discussion

In the present study, we obtained evidence of the involvement of BPMs in DREB2A degradation via the NRD, the molecular mechanism of which has remained unknown for a decade. The DREB2A protein is so unstable that it is difficult to achieve accumulation of DREB2A in plant cells under normal conditions even through overexpression of *DREB2A*. Although a previous domain analysis showed that deletion of the NRD transforms DREB2A into a stable form, known as DREB2A CA (10), the molecular basis of this phenomenon remained unclear. Thus, we isolated BPMs as novel interactors of DREB2A (Fig. 1 and Figs. S1 and S2 *E* and *F*) and found that BPMs degrade DREB2A in an N-NRD–dependent manner (Fig. 3 *C*–*E*), indicating involvement of the $CRL3^{BPM}$-mediated pathway in the destabilization of DREB2A via the NRD. Considering these findings together, we conclude that the recruitment of CRL3 via BPMs is the long-sought system underlying the NRD-dependent degradation of DREB2A.

The data obtained from the *amiBPM* plants highlight the importance of BPMs in the control of DREB2A stability. In protoplasts, knockdown of *BPMs* caused significant accumulation of DREB2A FL, even under normal conditions (Fig. 3 *D* and *E*). Considering the partial loss of BPM activity in this experiment (Fig. 3*A*), BPMs seem to play a crucial role in DREB2A degradation. Hyperaccumulation of DREB2A was also observed under both heat and drought stress conditions in *amiBPM* plants (Fig. 4 *A* and *B*). Furthermore, DREB2A protein levels remained almost constant in the *amiBPM* plants under heat stress conditions, even in the presence of CHX (Fig. 4*C*). These results clearly show that BPMs are the key players in the control of DREB2A stability under both control and stress conditions, particularly under heat stress. Thus, the NRD-mediated destruction of DREB2A via BPMs controls DREB2A protein levels, not only under normal conditions, but also in stress responses.

Transcriptomic and physiological analyses suggest that BPMs play an important role in modulation of the heat stress response through regulation of the DREB2A regulon. Gene expression analyses revealed that approximately one-half of the heat-inducible genes up-regulated in the *amiBPM* plants are under the control of DREB2A (Fig. 5*C*). These genes included *HsfA3* and *SRC2*, which are reportedly involved in the acquisition of thermotolerance and the activation of ROS signaling, respectively (Fig. 5 *A* and *D*) (27–29). Consistent with the induction of these genes, *amiBPM* plants exhibited higher thermotolerance on both agar plates and in soil (Fig. 6 *A*–*G*). These results indicate that BPMs negatively regulate the heat stress response specifically through the DREB2A pathway. This idea is strongly supported by genetic analysis with the *dreb2a* mutant, because *amiBPM*/*dreb2a* plants did not show an enhanced heat stress response (Fig. S5 B–E). Therefore, our present results indicate that $CRL3^{BPM}$ makes a critical contribution to controlling the heat stress response through the regulation of

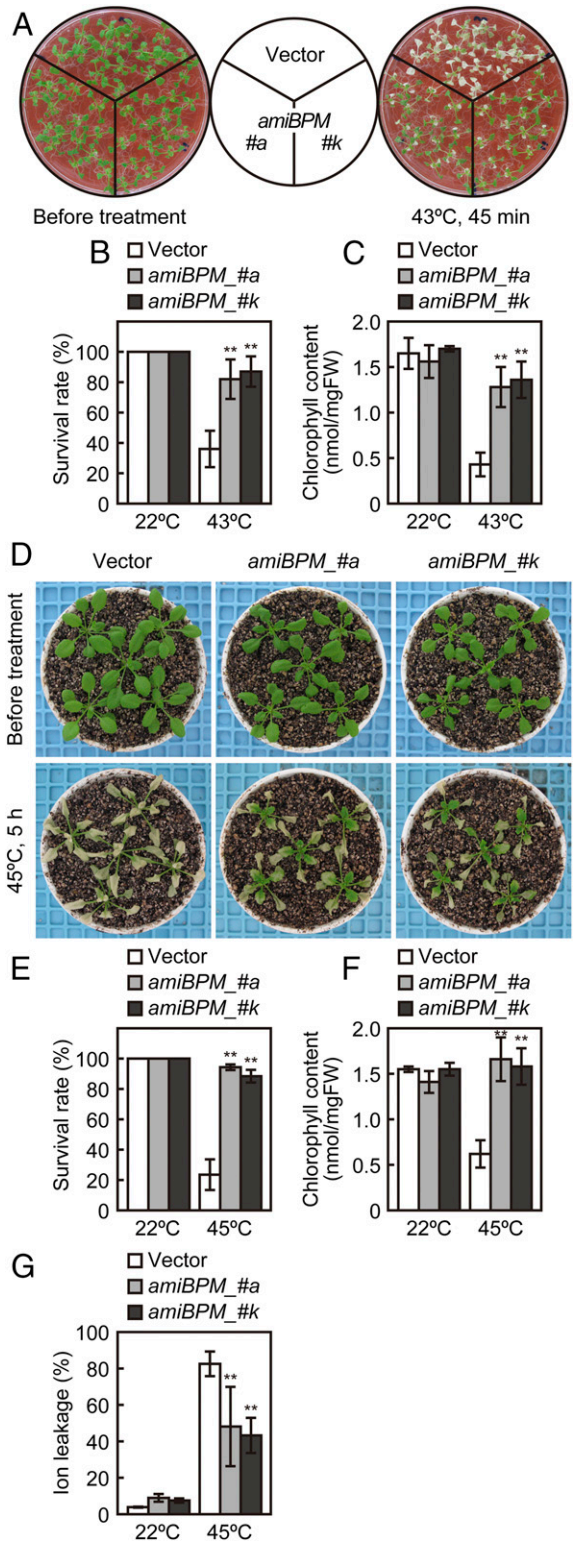

Fig. 6. Knockdown of *BPMs* confers thermotolerance. (*A*–*C*) Thermotolerance test of the *amiBPM* plants on agar plates. (*A*) Images of plants before (*Left*) and after (*Right*) heat shock (43 °C for 45 min). (*B*) Survival rate of the control (22 °C) and heat-stressed (43 °C) plants. The error bars indicate the SD from nine replicates ($n = 17$ each). Asterisks indicate significant differences between *amiBPM* and VC plants: $^{**}P < 0.01$, Student's *t* test. (*C*) Chlorophyll content of control and heat-stressed plants. The error bars indicate the SD from at least three replicates. Asterisks indicate significant differences between *amiBPM* and VC plants: $^{**}P < 0.01$, Student's *t* test. (*D*–*G*) Thermotolerance test of the *amiBPM* plants on soil. (*D*) Images of plants before (*Top*) and after (*Bottom*) heat shock (45 °C for 5 h). (*E*) Survival rates of control (22 °C) and heat-stressed (45 °C) plants. The error bars indicate the SD from three replicates ($n = 56$ total). Chlorophyll content (*F*) and ion leakage (*G*) of control and heat-stressed plants are shown with error bars indicating the SD from at least three replicates. Asterisks indicate significant differences between *amiBPM* and VC plants: $^{**}P < 0.01$, Student's *t* test.

DREB2A stability. In contrast, it is difficult to properly evaluate the effect of DREB2A stabilization on drought stress tolerance in *amiBPM* plants because BPMs also target ATHB6, a negative regulator of ABA signaling (18). As a result of ATHB6 accumulation, *BPM* knockdown causes disruption of stomatal closure and ABA-responsive gene expression, which negatively affect drought tolerance. Nonetheless, we compared the drought stress tolerance of *amiBPM* and VC plants and found that *BPM* knockdown decreased drought tolerance regardless of the up-regulation of *RD29B* and *GolS1* (Fig. 5*B* and Fig. S6 *A* and *B*). The negative effect of ATHB6 accumulation appears to cancel out the positive effect of DREB2A. Therefore, BPMs may regulate the strength of the drought stress response via the stability modulation of positive and negative regulators, depending on environmental conditions. To investigate this possibility and to fully understand the effect of BPM-mediated DREB2A degradation on drought tolerance, genetic analysis with *BPM* knockdown plants in the background of *athb6* knockout will be required in future analyses.

Our results suggest that $CRL3^{BPM}$ functions as the core system in achieving the rapid turnover of transcription factors. BPMs preferentially interact with transcription factors (17–19, 24). We observed that most BPM-interacting transcription factors possess SBC or SBC-like motifs (Fig. S2*C*). Interaction assays between mutated N-NRD and BPM2 strongly suggest that the SBC motif functions as a recognition sequence for BPMs (Fig. 2*B* and Fig. S2*B*), confirming the likelihood that BPM-interacting transcription factors are the true substrates of BPMs. Because transcription factors significantly impact the transcriptome and physiological status of plant cells, these proteins are generally unstable and require strict control at the protein level (30). Considering the ubiquitous expression of *BPMs* (24), $CRL3^{BPM}$-mediated degradation may be the general system for increasing the turnover of transcription factors. For example, several BPM interactors, such as DREB1A, ATHB6, and WIND1, are induced and play important roles in cold, ABA, and wounding responses, respectively (18, 31, 32); however, these transcription factors must be rapidly removed after stress responses, because the overaccumulation of these factors has negative effects on plant growth and productivity. In addition, other BPM interactors, such as ERF1, MYB56, and RAV1, are involved in the control of developmental processes (19, 33, 34). The accumulation of these proteins also must be strictly regulated depending on the transition of developmental stages to ensure proper growth. Therefore, BPMs may contribute to divergent cellular responses via the degradation of transcription factors to achieve appropriate transcriptional patterns throughout the life cycle.

We have shown that DREB2A stability is regulated via several distinct pathways. BPMs and DRIP1/2 function independently in DREB2A degradation (Fig. S3 *A*–*C*). In addition, RCD1 has been implicated in DREB2A degradation (20). Because the RCD1-binding site is located in the C-terminal region of DREB2A, there appear to be three different pathways involved in DREB2A degradation. Furthermore, BPMs and DRIP1/2 destabilize DREB2A continuously during stress responses (Fig. S4 *B* and *C*), indicating that the destruction of DREB2A is coupled with its synthesis. These findings imply that the rapid turnover of the DREB2A protein is constitutive. This idea is consistent with the potent destruction of DREB2A observed under normal conditions and during recovery from heat stress (13). Activation of the DREB2A regulon is important for plants to survive heat and drought stress conditions;

however, it is a trade-off between the acquisition of stress tolerance and growth (10). In nature, the degree of stress, along with the movement of sunlight, rainfall, or wind, occasionally changes in a short timeframe; therefore, negative regulation, such as DREB2A degradation, is an important stress response mechanism for plants to reduce inefficient energy use. The rapid turnover of DREB2A enables plants to quickly fine-tune DREB2A protein levels depending on the conditions, which may be important to the ability of plants to resiliently adapt to the changing environment, minimizing the negative effect of DREB2A on growth and productivity.

While the present study has revealed the mechanism of DREB2A degradation via the NRD, how DREB2A escapes proteolysis under stress conditions remains unclear. In addition, the activation mechanism of DREB2A remains elusive. In the case of WRI1, BPMs regulate not only the stability of this protein, but also its activity (17). The BPM-mediated regulation of DREB2A stability might be coupled with the regulation of DREB2A activity. We assume that unidentified DREB2A interactors modulate the stability and activity of DREB2A to escape the multiple associated degradation pathways, particularly $CRL3^{BPM}$-mediated degradation. Because the SBC motif contains serine and threonine residues, phosphorylation of the SBC motif appears to be a possible event altering the DREB2A–BPM interaction. Furthermore, DREB2A activity is differentially regulated depending on stress conditions, as DREB2A induces different sets of genes during heat and drought stress treatments (11). Therefore, in a condition-dependent manner, multiple factors may be involved in the stabilization and activation of DREB2A through the regulation of different processes. These complex regulatory mechanisms of DREB2A, considering its stabilization and activation under stress conditions, may be further clarified by considering the multiple degradation pathways of DREB2A.

Materials and Methods

Plant Materials, Growth Conditions, and Transformation. *Arabidopsis thaliana* (L.) Heynh. ecotype Columbia was used as the WT line. Transgenic plants overexpressing *GFP* or *GFP-DREB2A* in the background of *dreb2a* (GK_379F02) were generated as described previously (13). The *drip1 drip2* double mutant was reported previously (12). *Arabidopsis* plants were grown and transformed as described previously (12).

Abiotic Stress and Chemical Treatments. Plants used for abiotic stress and chemical treatments were grown on agar medium. For the abiotic stress treatments, 2-wk-old *Arabidopsis* seedlings were transferred to drought or heat stress conditions as described previously (10, 11). For MG132 treatment, 2-wk-old seedlings were placed in a Petri dish filled with distilled water containing MG132 (100 μM; Peptide Institute). For CHX treatment, 2-wk-old seedlings were placed in a Petri dish filled with distilled water and then incubated under the heat stress conditions for 3 h. Distilled water was replaced with prewarmed water containing CHX (200 μg/mL; Sigma-Aldrich), followed by continuous incubation under heat stress conditions.

In Vivo Cross-Linking and Immunoprecipitation. The 2-wk-old *Arabidopsis* seedlings were treated with 100 μM MG132 under heat stress conditions for 5 h to prevent degradation of the DREB2A protein. The plants were immersed in 10 volumes of 1 mM dithiobis(succinimidyl propionate) (DSP; Thermo Fisher Scientific), a membrane-permeable bifunctional cross-linker, and then vacuum-infiltrated for 5 min to fix a transient protein–protein interaction in intact plants. After vacuum infiltration, the samples were incubated for 30 min at room temperature. To quench cross-linking, Tris·HCl (pH 7.5) was added to a final concentration of 50 μM. After vacuum infiltration for 5 min, the samples were incubated for 15 min at room temperature. The cross-linked samples were subsequently ground into powder in liquid nitrogen and then homogenized in extraction buffer [20 mM Hepes-KOH (pH 7.6), 150 mM NaCl, 5 mM $MgCl_2$, 20% glycerol, 1% (vol/vol) Triton X-100, 0.02% (vol/vol) Tween 20, 0.1 mM EDTA, 0.02 mM MG132, and 1× cOmplete Protease Inhibitor Mixture (Roche)]. The total protein extract was then subjected to immunoprecipitation using the μMACS GFP Isolation Kit (Miltenyi Biotec) according to the manufacturer's instructions.

Peptide Preparation and LC-MS/MS Analysis. The immunoprecipitated DREB2A and copurified proteins were separated using SDS/PAGE. The resultant protein bands were visualized by silver staining using the Silver Stain MS Kit (Wako) and then excised for peptide preparation for LC-MS/MS analysis. The excised gel pieces were subjected to in-gel digestion with a mixture of trypsin and Lys-C (Trypsin/Lys-C Mix, Mass Spec Grade; Promega). The digested peptides were recovered by adding 50% (vol/vol) acetonitrile/5% (vol/vol) formic acid. LC-MS/MS analysis was performed using the AB SCIEX TripleTOF 5600 System. The MS/MS spectra were compared against TAIR10, and MS scores were calculated using the ProteinPilot server.

Immunoblot Analysis. Protein immunoblot analyses were conducted as described previously (13). For the detection of proteins, the primary antibodies were anti-DREB2A (13), anti-GFP (35), anti-FLAG (Sigma-Aldrich), and anti-GST-tag pAb-HRP-DirecT (MBL), and the secondary antibody was horseradish peroxidase-conjugated anti-rabbit IgG or anti-mouse IgG (Sigma-Aldrich). The signal was developed using ECL Prime (GE Healthcare) according to the manufacturer's instructions and detected with an ImageQuant LAS-4000 biomolecular imager (GE Healthcare).

Y2H Assays. Y2H assays were performed using the MatchMaker GAL4 Two-Hybrid System 3 (Clontech) according to the manufacturer's instructions. The yeast strain AH109 was transformed with pairs of pGBKT7- and pGADT7-based plasmids harboring genes of interest. The transformants were grown on synthetic dropout (SD) agar or liquid medium lacking Leu and Trp (–LW) or SD medium lacking Leu, Trp, His, and adenine (–LWHA). β-galactosidase assays were performed according to the Yeast Protocols Handbook (Clontech).

Pull-Down Assay. Recombinant proteins were expressed in *Escherichia coli* (Rosetta [DE3] pLys) and affinity-purified with glutathione Sepharose 4B (GE Healthcare Life Sciences) or HisPur cobalt resin (Life Technologies) according to the manufacturer's instructions. The proteins were mixed and incubated in binding buffer (50 mM Tris·HCl pH 7.5, 150 mM NaCl, 5 mM $MgCl_2$, 0.2% Nonidet P-40, and 10% glycerol). The protein complexes were recovered using glutathione Sepharose 4B beads and eluted with 1× Laemmli buffer after boiling at 95 °C for 3 min.

Transient Expression in *Arabidopsis* Mesophyll Protoplasts. Protoplast isolation and transfection were performed as described previously (36). For the reporter assays and immunoblot analysis, a plasmid mixture containing an internal control plasmid for the reporter assays (pBI35SΩELUC), an internal control plasmid for immunoblot analysis (pGKX-NsGFP), a reporter plasmid (DRE×3-GUS), and an effector plasmid was used for transfection. Transfected protoplasts were divided into two aliquots, and each aliquot was used for reporter assays and immunoblot analyses. Reporter and immunoblot assays with protoplasts were performed as described previously (37).

Transient Expression in Onion Epidermal Cells. Onion epidermal cells were transformed using the particle bombardment method with the PDS-1000/He system (Bio-Rad) according to the manufacturer's instructions. For the observation of subcellular localization, pGKX-NsGFP–based plasmids were used for transformation. For the BiFC assays, a plasmid mixture containing pSPYNE(R)173- and pSPYCE(M)-based plasmids (38) and a transformation control plasmid (pGKX-CFP) was used for transformation.

Fluorescence Observations. Fluorescence images of CFP, GFP, and YFP were obtained using a confocal laser-scanning microscope (LSM 5 PASCAL; Carl Zeiss) with the following filters: a 458-nm excitation filter and BP470 500-nm emission filter for CFP fluorescence, a 488-nm excitation filter and BP505 530-nm emission filter for GFP fluorescence, and a 488-nm excitation filter and BP530 600-nm emission filter for YFP fluorescence.

Total RNA Extraction and qRT-PCR. Total RNA isolation and qRT-PCR were performed as described previously (12). The primers used for qRT-PCR are listed in Table S1. Similar results were obtained in two independent experiments. *P* values were corrected with the Bonferroni method.

Microarray Analysis and Data Processing. Transcriptome analysis was performed with an *Arabidopsis* 3 Oligo Microarray (Agilent Technologies) as described previously (39). RNA was extracted from 2-wk-old seedlings of VC and *amiBPM* plants treated with heat stress at 37 °C for 5 h. Data analyses were performed as described previously (26). All microarray data are available at Array Express (accession no. E-MTAB-5845).

Thermotolerance Test. The thermotolerance test on agar plates was performed as described previously, with some modifications (37). Two-week-old seedlings were exposed to heat stress at 43 °C for 45 min. After a 1-wk recovery period, images of the plants were captured, and survival rates were determined. The viable plants were defined as those that remained green after recovery. For the thermotolerance test on soil, 2-wk-old seedlings grown on agar plates were transferred to soil pots. After 1 wk, the plants were exposed to heat stress at 45 °C for 5 h. During this treatment and subsequent recovery, the plants were covered with plastic wrap to keep the humidity high. After recovery for 2 d, images of the plants were captured, and survival rates were determined. Viable plants were defined as those that maintained a green shoot apical meristem.

Measurement of Chlorophyll Content. Chlorophyll was extracted from heat-stressed plants after recovery for 1 wk (agar plate) or 2 d (soil). Ground samples were homogenized in 80% acetone and incubated overnight in the dark. Extracted chlorophyll was quantified as described previously (40).

Measurement of Ion Leakage. Ion leakage was measured from heat-stressed plants after recovery for 1 wk (agar plate) or 2 d (soil). Plants were immersed in water and shaken overnight in the dark. After measurement of the electric conductivity (EC1) with a LAQUA Twin meter (Horiba), the samples were frozen in liquid nitrogen and shaken overnight in the dark again. After measurement of the electric conductivity (EC2), the ion leakage was calculated as the value of EC1/EC2.

Drought Tolerance Test. Two-week-old seedlings grown on agar plates were transferred to soil pots. After 2 d, dehydration was initiated by withholding water for 2 wk. After 5 d of recovery following rehydration, images were captured, and survival rates were determined. Viable plants were defined as those that generated new leaves during recovery.

Plasmid Construction. For Y2H assays, the PCR products of the RCD1, SAP18, TCP1, BPM1, BPM2, BPM3, BPM4, BPM5, BPM6, DREB2A, and DREB2A fragments were cloned into pGBKT7 and pGADT7 plasmids through restriction digestion. BPM2 ΔMATH and BPM2 ΔBTB were generated via inverse PCR. The GFP fusion constructs for use in plant transformation and transient expression in onion cells were generated by cloning the PCR products of BPM2 and BPM4 into the pGKX-NsGFP plasmid through restriction digestion. pGKX-NsGFP-DREB2A was generated in a previous study (10). For the BiFC assay, the PCR products of BPM1, BPM2, BPM3, BPM4, BPM5, and BPM6 were cloned into pSPYCE(M) plasmids through restriction digestion. BTB domain-lacking forms of each BPM were generated through inverse PCR. DREB2A was cloned into the pSPYNE(R)173 plasmid. To generate the expression vector for *E. coli*, BPM2 was cloned into the pCold GST plasmid (37). The Trx-His-DREB2A expression plasmid was generated in a previous study (12). To generate the amiRNA-expressing construct, primers were designed with WMD3-Web MicroRNA Designer, and the amiRNA precursor was constructed using the WMD3-Web MicroRNA Designer website. The precursor was cloned into the pGKX plasmid for transformation. The primers and cloning information used are specified in Table S1.

ACKNOWLEDGMENTS. We thank Y. Tanaka and S. Murasaki for excellent technical support and E. Toma for skillful editorial assistance. This work was supported through Grants-in-Aid from the Ministry of Education, Culture, Sports, Science and Technology of Japan for Research Activity Startup (16H06735, to N.O.) and for Scientific Research on Innovative Areas (15H05960, to K.Y.-S.), and the Program for the Promotion of Basic Research Activities for Innovative Biosciences of Japan (to K.S. and K.Y.-S.).

1. Yamaguchi-Shinozaki K, Shinozaki K (2006) Transcriptional regulatory networks in cellular responses and tolerance to dehydration and cold stresses. *Annu Rev Plant Biol* 57:781–803.
2. Ohama N, Sato H, Shinozaki K, Yamaguchi-Shinozaki K (2017) Transcriptional regulatory network of plant heat stress response. *Trends Plant Sci* 22:53–65.
3. Covarrubias AA, Reyes JL (2010) Post-transcriptional gene regulation of salinity and drought responses by plant microRNAs. *Plant Cell Environ* 33:481–489.
4. Miura K, Hasegawa PM (2010) Sumoylation and other ubiquitin-like post-translational modifications in plants. *Trends Cell Biol* 20:223–232.
5. Lyzenga WJ, Stone SL (2012) Abiotic stress tolerance mediated by protein ubiquitination. *J Exp Bot* 63:599–616.
6. Meng X, Zhang S (2013) MAPK cascades in plant disease resistance signaling. *Annu Rev Phytopathol* 51:245–266.
7. Nakashima K, Ito Y, Yamaguchi-Shinozaki K (2009) Transcriptional regulatory networks in response to abiotic stresses in *Arabidopsis* and grasses. *Plant Physiol* 149:88–95.
8. Kim J-S, et al. (2011) An ABRE promoter sequence is involved in osmotic stress-responsive expression of the DREB2A gene, which encodes a transcription factor regulating drought-inducible genes in *Arabidopsis*. *Plant Cell Physiol* 52:2136–2146.
9. Yoshida T, et al. (2011) *Arabidopsis* HsfA1 transcription factors function as the main positive regulators in heat shock-responsive gene expression. *Mol Genet Genomics* 286:321–332.
10. Sakuma Y, et al. (2006) Functional analysis of an *Arabidopsis* transcription factor, DREB2A, involved in drought-responsive gene expression. *Plant Cell* 18:1292–1309.
11. Sakuma Y, et al. (2006) Dual function of an *Arabidopsis* transcription factor DREB2A in water-stress-responsive and heat-stress-responsive gene expression. *Proc Natl Acad Sci USA* 103:18822–18827.
12. Qin F, et al. (2008) *Arabidopsis* DREB2A-interacting proteins function as RING E3 ligases and negatively regulate plant drought stress-responsive gene expression. *Plant Cell* 20:1693–1707.
13. Morimoto K, et al. (2013) Stabilization of *Arabidopsis* DREB2A is required but not sufficient for the induction of target genes under conditions of stress. *PLoS One* 8:e80457.
14. Zimmerman ES, Schulman BA, Zheng N (2010) Structural assembly of cullin-RING ubiquitin ligase complexes. *Curr Opin Struct Biol* 20:714–721.
15. Hua Z, Vierstra RD (2011) The cullin-RING ubiquitin-protein ligases. *Annu Rev Plant Biol* 62:299–334.
16. Gingerich DJ, et al. (2005) Cullins 3a and 3b assemble with members of the broad complex/tramtrack/bric-a-brac (BTB) protein family to form essential ubiquitin-protein ligases (E3s) in *Arabidopsis*. *J Biol Chem* 280:18810–18821.
17. Chen L, et al. (2013) *Arabidopsis* BPM proteins function as substrate adaptors to a cullin3-based E3 ligase to affect fatty acid metabolism in plants. *Plant Cell* 25:2253–2264.
18. Lechner E, et al. (2011) MATH/BTB CRL3 receptors target the homeodomain-leucine zipper ATHB6 to modulate abscisic acid signaling. *Dev Cell* 21:1116–1128.
19. Chen L, Bernhardt A, Lee J, Hellmann H (2015) Identification of *Arabidopsis* MYB56 as a novel substrate for CRL3(BPM) E3 ligases. *Mol Plant* 8:242–250.
20. Vainonen JP, et al. (2012) RCD1-DREB2A interaction in leaf senescence and stress responses in *Arabidopsis thaliana*. *Biochem J* 442:573–581.
21. Weber H, et al. (2005) *Arabidopsis* AtCUL3a and AtCUL3b form complexes with members of the BTB/POZ-MATH protein family. *Plant Physiol* 137:83–93.
22. Mori M, et al. (1992) Cloning of a cDNA encoding the Tcp-1 (t complex polypeptide 1) homologue of *Arabidopsis thaliana*. *Gene* 122:381–382.
23. Song CP, Galbraith DW (2006) AtSAP18, an orthologue of human SAP18, is involved in the regulation of salt stress and mediates transcriptional repression in *Arabidopsis*. *Plant Mol Biol* 60:241–257.
24. Weber H, Hellmann H (2009) *Arabidopsis thaliana* BTB/ POZ-MATH proteins interact with members of the ERF/AP2 transcription factor family. *FEBS J* 276:6624–6635.
25. Zhuang M, et al. (2009) Structures of SPOP-substrate complexes: Insights into molecular architectures of BTB-Cul3 ubiquitin ligases. *Mol Cell* 36:39–50.
26. Ogawa D, Yamaguchi K, Nishiuchi T (2007) High-level overexpression of the *Arabidopsis* HsfA2 gene confers not only increased themotolerance but also salt/osmotic stress tolerance and enhanced callus growth. *J Exp Bot* 58:3373–3383.
27. Schramm F, et al. (2008) A cascade of transcription factor DREB2A and heat stress transcription factor HsfA3 regulates the heat stress response of *Arabidopsis*. *Plant J* 53:264–274.
28. Yoshida T, et al. (2008) Functional analysis of an *Arabidopsis* heat-shock transcription factor HsfA3 in the transcriptional cascade downstream of the DREB2A stress-regulatory system. *Biochem Biophys Res Commun* 368:515–521.
29. Kawarazaki T, et al. (2013) A low temperature-inducible protein AtSRC2 enhances the ROS-producing activity of NADPH oxidase AtRbohF. Biochim Biophys Acta Mol *Cell Res* 1833:2775–2780.
30. Collins GA, Tansey WP (2006) The proteasome: A utility tool for transcription? *Curr Opin Genet Dev* 16:197–202.
31. Liu Q, et al. (1998) Two transcription factors, DREB1 and DREB2, with an EREBP/AP2 DNA binding domain separate two cellular signal transduction pathways in drought- and low-temperature-responsive gene expression, respectively, in *Arabidopsis*. *Plant Cell* 10:1391–1406.
32. Iwase A, et al. (2011) The AP2/ERF transcription factor WIND1 controls cell dedifferentiation in *Arabidopsis*. *Curr Biol* 21:508–514.
33. Mao JL, et al. (2016) *Arabidopsis* ERF1 mediates cross-talk between ethylene and auxin biosynthesis during primary root elongation by regulating ASA1 expression. *PLoS Genet* 12:e1005760.
34. Woo HR, et al. (2010) The RAV1 transcription factor positively regulates leaf senescence in *Arabidopsis*. *J Exp Bot* 61:3947–3957.
35. Tanaka H, et al. (2012) Abiotic stress-inducible receptor-like kinases negatively control ABA signaling in *Arabidopsis*. *Plant J* 70:599–613.
36. Yoo S-D, Cho Y-H, Sheen J (2007) *Arabidopsis* mesophyll protoplasts: A versatile cell system for transient gene expression analysis. *Nat Protoc* 2:1565–1572.
37. Ohama N, et al. (2016) The transcriptional cascade in the heat stress response of *Arabidopsis* is strictly regulated at the level of transcription factor expression. *Plant Cell* 28:181–201.
38. Waadt R, et al. (2008) Multicolor bimolecular fluorescence complementation reveals simultaneous formation of alternative CBL/CIPK complexes in planta. *Plant J* 56:505–516.
39. Mizoi J, et al. (2013) GmDREB2A;2, a canonical DEHYDRATION-RESPONSIVE ELEMENT-BINDING PROTEIN2-type transcription factor in soybean, is posttranslationally regulated and mediates dehydration-responsive element-dependent gene expression. *Plant Physiol* 161:346–361.
40. Porra RJ, Thompson WA, Kriedemann PE (1989) Determination of accurate extinction coefficients and simultaneous equations for assaying chlorophyll-a and chlorophyll-b extracted with 4 different solvents: Verification of the concentration of chlorophyll standards by atomic-absorption spectroscopy. *Biochim Biophys Acta* 975:384–394.